Journal of Nuclear Materials 406 (2010) 251–256

Contents lists available at ScienceDirect

Journal of Nuclear Materials

journal homepage: www.elsevier.com/locate/jnucmat

Understanding silicon-rich phase precipitation under irradiation in austenitic stainless steels

A. Etienne *, B. Radiguet, P. Pareige

Groupe de Physique des Matériaux, Université et INSA de Rouen, UMR CNRS 6634, BP 12, 76 801 Saint Etienne du Rouvray Cedex, France

ARTICLE INFO

Article history:
Received 12 July 2010
Accepted 28 August 2010

ABSTRACT

Atom probe samples have been Fe^+ ion irradiated at different doses (from 0.5 to 10 dpa) and different temperatures (between 300 and 400 °C) in order to understand the mechanism of formation, under irradiation, of Si-rich phases in austenitic stainless steels. Atom probe results show the presence of Si-enriched clusters which can also be enriched in Ni and depleted in Cr. Number densities of solute clusters can be linked to number densities of dislocation loops already observed by transmission electron microscopy in a previous work. This suggests that solute clusters are formed by heterogeneous precipitation on dislocation loops. Furthermore, the evolution of the composition of solute clusters as a function of the irradiation temperature is consistent with a radiation-induced mechanism. Results are also compared with previous results obtained after neutron irradiation at lower dose rate (in term of dpa s^{-1}). The comparison is, here again, consistent with the radiation-induced mechanism. Thus, Si-rich clusters may be formed by radiation-induced segregation to dislocation loops. Results also show that Si is probably dragged to sinks via the interstitial mechanism.

1. Introduction

The internal structures of pressurized water reactors (PWR) located close to the reactor core consist generally of baffle plates made of solution annealed 304 stainless steel (SS) and bolts made of cold worked 316SS. They are exposed to a high dose neutron irradiation (up to 80 dpa after 30 years of reactor service) at temperatures between 300 °C and 380 °C. This irradiation is known to induce a reduction of ductility and an overall hardening, i.e. an increase of the yield stress. This evolution is associated with the accumulation of the irradiation damage, mainly Frank dislocation loops, which act as obstacles to the motion of dislocations [1–5]. The radiation-induced hardening is held responsible for the degradation of material properties and contributes to the stress corrosion cracking [6]. Since the evolution of the macroscopic properties is related to the evolution of the microstructure, understanding the microstructure evolution under irradiation is essential to predict time-of-life of internals. Thus, since the last 15 years a large number of studies have focused on the characterization of these microstructures under irradiation. On the one hand, a part of them covers the radiation-induced segregation (RIS) at grain boundaries (GB), known to play a role in the loss of corrosion resistance and in the irradiation assisted stress corrosion cracking (IASCC) [7–14]. On the other hand, transmission electron microscopy (TEM) observations have shown that the radiation hardening could be caused by the formation of a high density of Frank loops (faulted loops with a Burgers vector $a_0/3\langle 1\,1\,1\rangle$ lying in {1 1 1} planes) and point defects clusters [15–20]. In addition, phase transformations or solute segregation inside grains are also mentioned. Whereas no precipitation at the PWR irradiation temperature is expected, few examples of precipitation are reported under irradiation at temperatures below 400 °C. Carbide precipitation, γ' precipitation or Ni–Si enrichment at Frank loops are reported in Refs. [21–26]. Quantitative experimental results on the description of these nanostructures are rare for PWR ageing conditions. Recently, an atom probe tomography (APT) characterization of a 316SS, irradiated with neutrons in real PWR service conditions, has shown the formation of a high number density of Ni–Si clusters [27]. A mechanism of radiation-induced segregation on Frank loops has been suggested by the authors.

The aim here is to reproduce and understand the nanophase transformation by the use of model ion irradiations. APT is used for the characterization of the solute distribution. Results are compared with TEM results about Frank loop population, on the same material irradiated in similar conditions. The complementarity of these two experimental techniques is used to determine the formation mechanism of these nanophases.

Material characteristics and experimental procedure are given in the first part of this paper. Results are described and discussed in the second part.

* Corresponding author. Tel.: +33 2 32 95 51 40; fax: +33 2 32 95 50 32.
E-mail address: auriane.etienne@univ-rouen.fr (A. Etienne).

0022-3115/$ - see front matter © 2010 Elsevier B.V. All rights reserved.
doi:10.1016/j.jnucmat.2010.08.045

Table 1
Bulk composition of the 316SS samples. Balance is iron. Values are given both in atomic and weight percents.

	C	P	Si	Cr	Ni	Mo	Mn	Cu	Co
wt.%	0.054	0.027	0.68	16.60	10.60	2.25	1.12	0.24	0.12
at.%	0.25	0.048	1.34	17.70	10.02	1.30	1.13	0.21	0.11

Table 2
Irradiation conditions of atom probe and TEM samples.

Dose (dpa)	Technique	Flux (10^{14} ions m^{-2} s^{-1})	Dose rate (10^{-4} dpa s^{-1})	Irradiation temperature (°C)
0.5	APT	6.2	1.15	350
1	APT	6.2	1.15	350
5	APT/TEM	15.6	2.9	350
0.36	TEM	35	6.5	350
1	TEM	15.6	2.9	350
1.25	TEM	35	6.5	350
10	APT	28.5	5.3	300
5	APT	15.6	2.9	400

2. Experimental

The material investigated is a 300 series SS commonly used for core internals of PWR nuclear power plant namely a cold worked 316SS used for PWR bolts. Its bulk chemical composition is given in Table 1. It is 15% cold worked, fully austenitic, with a grain size of about 40 μm. Solute atoms are homogeneously distributed into austenitic grains [27]. The microstructure contains numerous dislocations organized in cells and deformation twins.

Rods of 10 mm long and 0.3 × 0.3 mm^2 in section, and disks of 3 mm in diameter were cut in order to prepare atom probe and TEM samples respectively. Atom probe samples (tip with an end radius smaller than 50 nm) were obtained by electropolishing rods at about 10 V in a solution of 98% butoxyethanol and 2% perchloric acid. Thin foils were obtained by mechanical thinning of the disks down to 100 μm, followed by electropolishing. Two different electrolytes were used for TEM sample preparation. The first is a solution of 70% of ethanol, 20% of 2-butoxyethanol and 10% perchloric acid and the second is a solution of 5% perchloric acid in methanol.

Already prepared APT thin needles and TEM thin foils were irradiated with 160 keV Fe^+ ions. The depth of implantation of iron ions with this energy is around 50 nm, that is to say the centre of an atom probe needle or of a TEM thin foil. TEM samples were irradiated in the ion implantor IRMA at the Centre de Spectrométrie Nucléaire et de Spectrométrie de Masse (CSNSM Orsay – France) [28] and in a similar one at the University Complutense at Madrid [29]. Atom probe samples were irradiated in a similar implantor located at the department "Physique et Mécanique des Matériaux" at the P' Institute (ex PHYMAT) at Poitiers – France. Irradiation conditions for both kinds of samples are reported in Table 2. The dose in displacement per atom (dpa) is estimated using SRIM 2006 [30] and the Kinchin Pease approximation [31]. As far as APT samples are concerned, irradiation doses are between 0.5 and 10 dpa for the lowest and the highest. Three different irradiation temperatures, from 300 °C to 400 °C, were used. In the case of TEM samples, doses are between 0.36 and 5 dpa and all irradiations were performed at 350 °C. It should be noticed that even if the dose rate in not exactly the same in each case, it is always in the range 10^{-4} dpa s^{-1}. There is a factor 5 between the highest and the lowest dose rate. Such difference is not high enough to result in significant flux effect.

APT experiments were performed using a Laser Assisted Tomographic Atom Probe (LATAP – Cameca) and a Laser Assisted Wide Angle Tomographic Atom Probe (LAWATAP – Cameca) [32,33]. Analyses were performed at 80 K, using green (λ = 515 nm) femtosecond laser pulses. The equivalent pulse fraction was estimated to be 20% for all samples. Details of TEM experiments are given in [34].

3. Results and discussion

3.1. Ion irradiations at 350 °C

After ion irradiation at 0.5 dpa, statistical tests show that silicon and nickel atoms are not randomly distributed. Statistical tests show that other species, as Mo and Cr, are randomly distributed. Experimental frequency distribution of Si atoms, depicted in Fig. 1, compared to a random distribution, shows the presence of Si enriched zones. These zones correspond to Si concentration fluctuations through which concentration profiles are plotted (Fig. 2). Si concentration reaches about 10 at.%. It is a local enrichment by a factor 6. No other solute enrichment or depletion is associated to these fluctuations. The size of theses Si enrichments is in the range of 1–2 nm in diameter and they are present with a number density of about (7 ± 6) × 10^{22} m^{-3}.

After irradiation up to 1 dpa, Si atoms are still distributed in a heterogeneous way and some Si enrichments are still visible. They

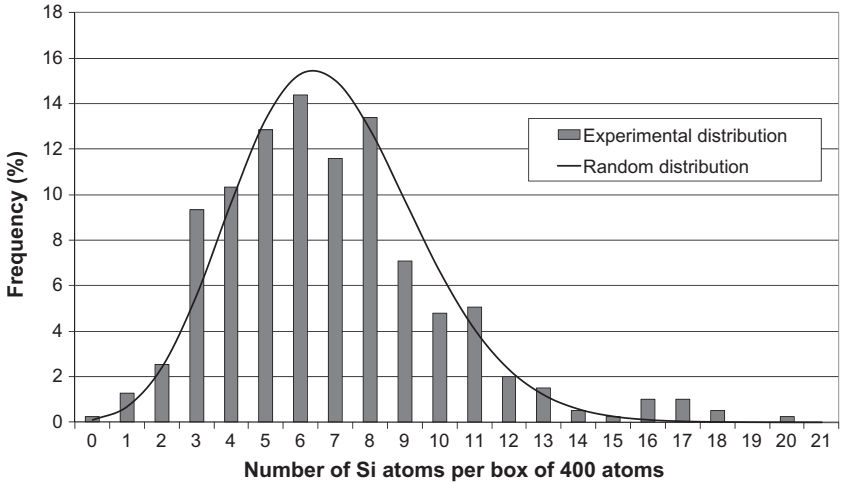

Fig. 1. Experimental frequency distribution of Si atoms in the 316SS sample irradiated at 0.5 dpa at 350 °C compared to a random distribution.

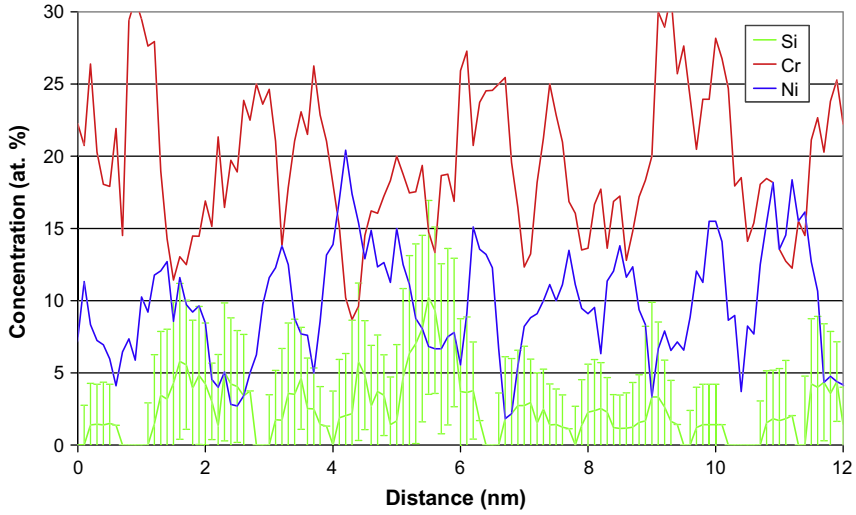

Fig. 2. Concentration profiles through a Si concentration fluctuation in a 316SS sample irradiated at 0.5 dpa at 350 °C. Only Si, Ni and Cr profiles are depicted.

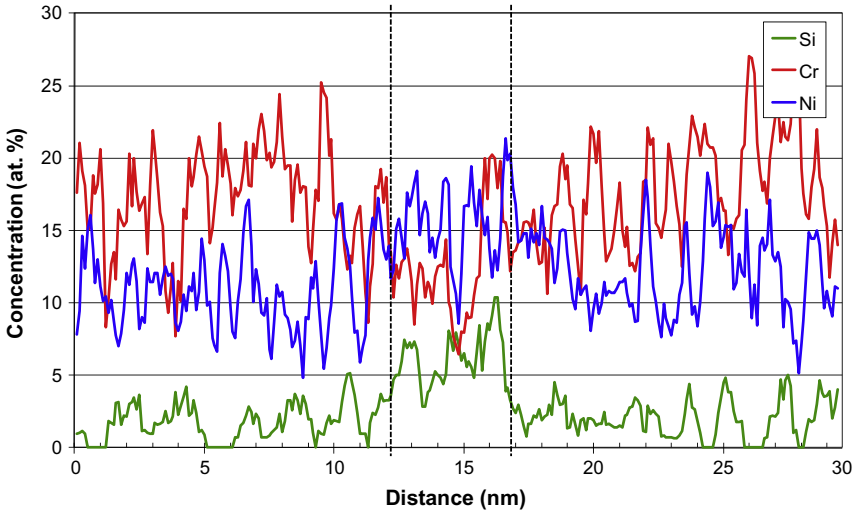

Fig. 3. Concentration profiles through a Si concentration enrichment in a 316SS sample irradiated at 1 dpa at 350 °C. Only Si, Ni and Cr profiles are depicted.

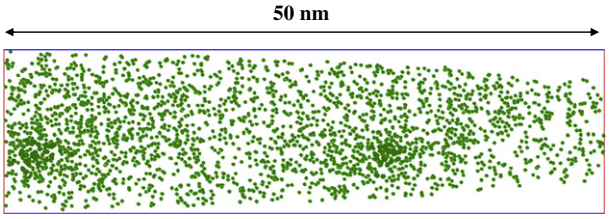

Fig. 4. 3D reconstruction of an of 316SS ion irradiated at 5 dpa at 350 °C. Only Si atoms are represented. Si atoms, in regions where the Si concentration is higher than 4 at.%, are emphasized.

are present with a number density of $(3 \pm 2) \times 10^{22}$ m^{-3}. Concentration profiles plotted through a Si enrichment are depicted in Fig. 3. The maximum Si concentration reaches, as previously, about 10 at.%. The average Si concentration in Si enrichment is 7.2 at.%. Combined with this enrichment of Si, an increase of Ni concentration and a decrease of Cr concentration are visible. The average Cr concentration is 13.9 at.% while the average Ni concentration is 14.8 at.%.

The same trend is observed after ion irradiation at 5 dpa. Si clusters, clearly visible in the analysed volume (Fig. 4) are enriched with Ni and depleted with Cr. Their number density is $(1.3 \pm 0.6) \times 10^{23}$ m^{-3}. Enrichment factors (ratio of the concentration in solute clusters over the matrix concentration) of solute clusters, given in Table 3, do not change for doses higher than 1 dpa.

In this way, after ion irradiation, same trends, that is to say enrichments in Ni and Si and a depletion in Cr, as observed in neutron irradiated samples [27], are found. Obviously, as ion irradiation conditions are different from PWR irradiation conditions, size and composition of clusters are different. This point is discussed later.

TEM experiments, which results are fully described in [34], show the presence of dislocation loops from the lowest dose. Size and number density of dislocation loops as a function of dose are depicted in Fig. 5. They are compared with size and number density of solute clusters observed by APT. The size of dislocation loops increases from 5 nm at 1 dpa to 9 nm for higher doses. The size of solute clusters increases from 1 nm at 0.5 dpa to 3 nm at 10 dpa. Whereas a factor of 4 appears between sizes of both kinds of ob-

Table 3
Si, Ni and Cr enrichment factors of solute clusters in Fe^+ irradiated and neutron irradiated 316SS.

	Dose (dpa)	Temperature (°C)	F (Si)	F (Ni)	F (Cr)
Fe^+ irradiation	0.5	350	6.2 ± 4.0	0.9 ± 0.6	1.0 ± 0.4
	1	350	4.0 ± 2.1	1.3 ± 0.4	0.8 ± 0.3
	5	350	5.4 ± 1.0	1.4 ± 0.2	0.85 ± 0.1
	10	300	5.9 ± 2.2	1.1 ± 0.4	0.9 ± 0.1
	5	400	7.0 ± 0.7	1.4 ± 0.1	0.75 ± 0.1
Neutron irradiation	12	360	56 ± 8	5.4 ± 0.4	0.06 ± 0.03

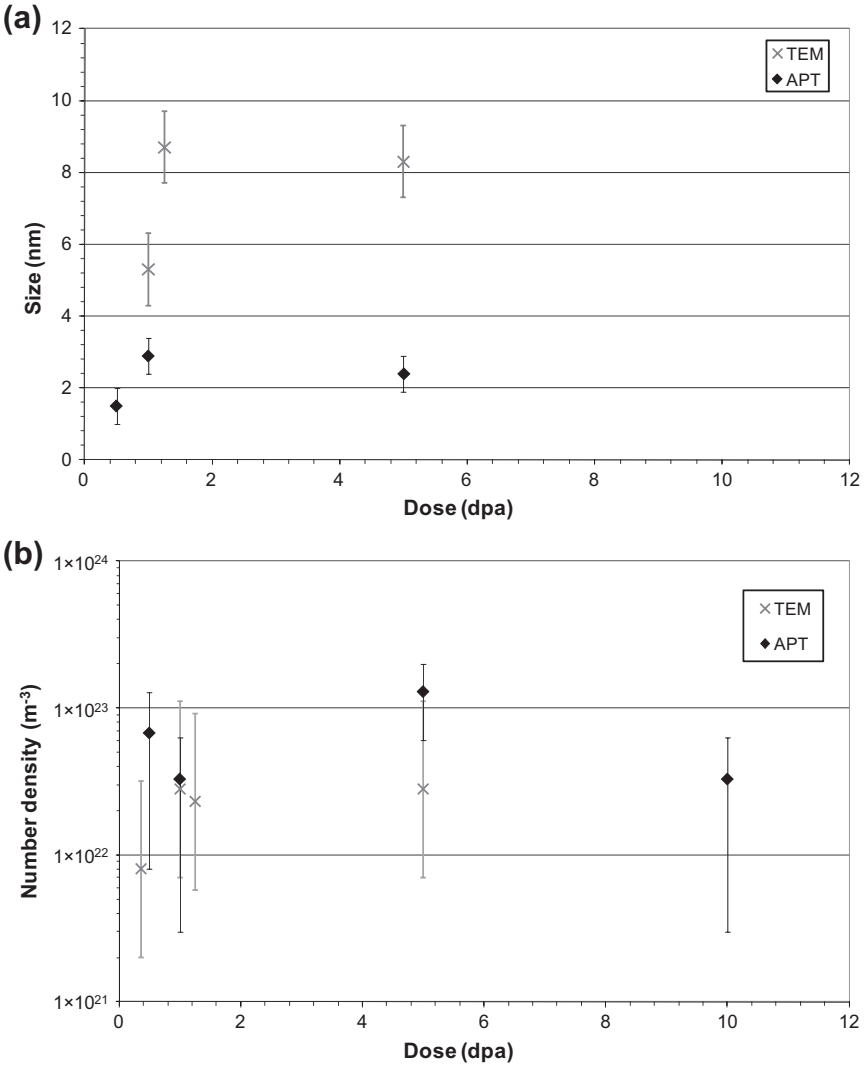

Fig. 5. (a) Dislocation loop size as a function of dose compared with solute cluster size and (b) dislocation loop density as a function of dose compared with solute cluster density.

jects, both densities are in the same order of magnitude, about 10^{22}–10^{23} m^{-3}. This correlation suggests a link between dislocation loops and solute clusters. Thus, solute clusters could be formed by heterogeneous precipitation on dislocation loops.

This hypothesis is supported by experimental observations in neutron irradiated austenitic stainless steels. Edwards et al. [35] show, in a 316SS irradiated at 25 dpa at 320 °C, the presence of an undefined fine scale precipitation with an average size of 5.7 nm and a number density of 10^{22} m^{-3}. The authors suggest a possible association of theses precipitates with dislocation loops. In addition, Kenik and Hojou [25] have observed in a nickel-stabilized austenite (USPCA), neutron irradiated up to 15 dpa at 520 °C, that large loops above 40 nm exhibited a significant Ni and Si enrichment up to 50 and 5 at.% respectively.

Considering the fact that the formation of Si clusters is due to a heterogeneous precipitation on dislocation loops, this mechanism can be accelerated or induced by irradiation. In order to gain insight, results obtained at 300 °C and 400 °C are considered.

3.2. Irradiations at 300 and 400 °C

At 300 °C, samples have been irradiated up to 10 dpa. Atom probe analyses still reveal the presence of Si clusters. They are only enriched in Si. Ni and Cr concentrations do not vary as it can be

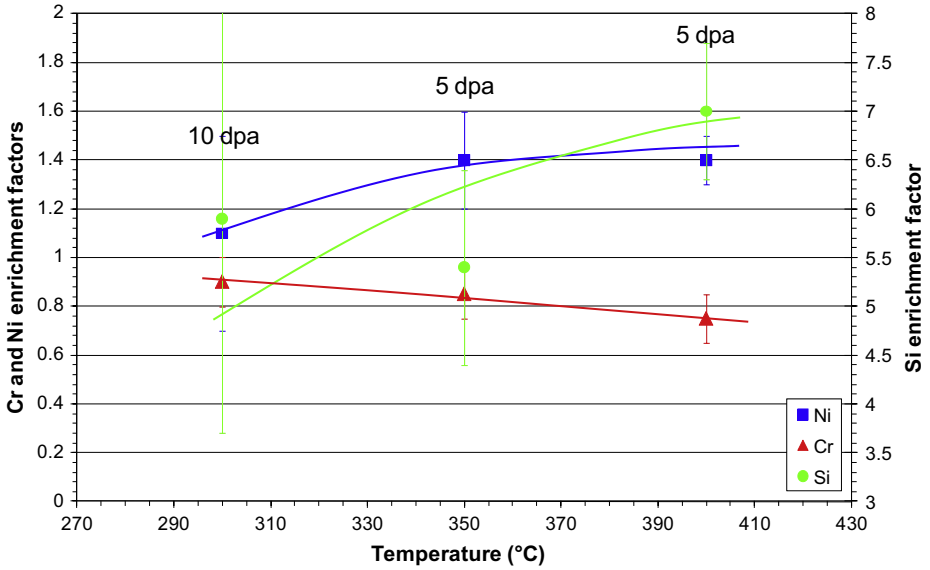

Fig. 6. Evolution of enrichment factors of Cr, Ni and Si of Si clusters as a function of the irradiation temperature.

seen in Table 3. Thus, these clusters are similar with those observed at 350 °C at the lowest dose.

In samples irradiated at 5 dpa at 400 °C, Si clusters exhibit enrichment in Ni and depletion in Cr. Enrichment factors, reported in Table 3, are slightly higher than those found after irradiation at 350 °C.

Evolution of enrichment factors of Si clusters as a function of the irradiation temperature is depicted in Fig. 6. As results at 350 °C show that cluster enrichment factors are stable for doses higher than 1 dpa, enrichment factors plotted on Fig. 6 are supposed to be saturation enrichment factors. Ni and Si enrichments and Cr depletion increase as the irradiation temperature increases. This trend is the same as what was observed in radiation-induced segregation at grain boundaries studies. Indeed, the intensity of radiation-induced segregation depends, at a given dose rate, on the irradiation temperature. As described by Allen et al. [36], at these relatively low temperatures, intensity of RIS increases as the temperature increases. This observation suggests that the mechanism of formation of Si clusters is induced by irradiation.

Thus, considering all the observations on TEM and APT samples irradiated with ions, the mechanism of formation of Si and Ni enriched clusters is likely radiation-induced segregation on dislocation loops. This conclusion is also supported by the fact that clusters are first enriched in Si. Cr depletion and Ni enrichment occur later. As mentioned by several studies [9,16], Si can be dragged to sinks, such as dislocation loops, via an interstitial mechanism, which is faster than the vacancy mechanism. Thus if Cr and Ni segregate by a vacancy mechanism, they reach or leave dislocation loops later. It should be noted that studies on RIS at grain boundaries do not show an early and unique Si segregation. However, this can be explained in two different ways. There are only few results dealing with quantitative Cr, Ni and Si RIS at grain boundaries at very low doses (0.5 dpa or less). In this study, the segregation of Si alone has been observed at 0.5 dpa. Results found in the literature are usually for doses higher than 0.5 dpa. Secondly, it is well know that, due to long-range elastic interactions, dislocations are a stronger sink for self interstitial atoms than for vacancies, which is not the case at grain boundaries. Considering that Si atoms segregate by the interstitial mechanism can explain that the early Si segregation is more pronounced at dislocation loops, and thus more easily observable than at grain boundaries.

This radiation-induced mechanism can also explain the differences between ion and neutron irradiations. As it was reported previously, the clusters observed after neutron irradiation [27] differ from the ones shown in this work. In neutron irradiated samples ($\sim 10^{-8}$ dpa s^{-1} at 360 °C), enrichment factors of Si and Ni reach respectively 56 and 5.4 which is ten times and five times higher than observed after ion irradiation ($\sim 10^{-4}$ dpa s^{-1} at 350 °C). In parallel, the enrichment factor of Cr is 0.06 which is more than ten times lower than in ion irradiated samples. It must be mentioned that the doses are not the same in both cases, 10 dpa and 5 dpa, for neutron and ion irradiations, respectively. However, as already mentioned, cluster composition is stationary between 1 and 5 dpa in the case of ions. So enrichment factors can be compared. It is well-known that at a given temperature, the RIS intensity depends on dose rate: for intermediate temperatures, lower the dose rate, higher the intensity of RIS [36,37]. Since dose rate is 10^4 times smaller in the case of neutron irradiation, a higher RIS intensity is expected, which correspond to experimental observations.

4. Conclusion

TEM and APT specimens of 316SS were irradiated with Fe^+ ions at various doses and temperatures in order to understand the mechanism of formation of Si-rich phase.

TEM and APT show respectively, the formation of Frank loops and solute clusters enriched in Si and, in some cases also enriched in Ni and depleted in Cr.

The irradiation kinetics, between 0.5 and 5 dpa, at 350 °C shows:

- A correlation between number densities of dislocation loops and solute clusters. This result suggests that the formation of solute clusters is heterogeneous on dislocation loops.
- Solute clusters are first enriched in Si. This observation supports the fact that Si atoms are dragged to sinks by an interstitial mechanism.
- The composition of solute clusters is stable for doses higher than 1 dpa.

Results obtained at 300 and 400 °C show that enrichment factors of solute clusters depend on the irradiation temperature. The

higher the irradiation temperature is, the higher the enrichment factors are. This trend is consistent with a radiation-induced mechanism.

Thus, solute clusters, observed in APT, are likely formed by radiation-induced segregation on Frank loops. This mechanism can also explain the difference in cluster composition measured after ion or neutron irradiation.

Acknowledgements

This work is a part of the research program of the EDF–CNRS joint laboratory EM^{2}VM (Study and Modelling of the Microstructure for Ageing of Materials).

The authors are grateful to Odile Kaitasov (CSNSM laboratory at Orsay – France), to Michel Drouet (PHYMAT laboratory at Poitiers – France) and to Pablo Fernández (University Complutense of Madrid – Spain) for performing ion irradiations.

Cécile Genevois and Mercedes Hernandez Mayoral are deeply acknowledged for their assistance in transmission electron microscopy works [34].

References

[1] M.L. Grossbeck, P.J. Maziasz, A.J. Rowcliffe, J. Nucl. Mater. 191 (1992) 808.
[2] G.R. Odette, D. Frey, J. Nucl. Mater. 85 (1979) 817.
[3] F. Garner, M.L. Hamilton, N.F. Panayotou, G.D. Johnson, J. Nucl. Mater. 103 (1981) 803.
[4] N. Yoshida, H.L. Heinisch, T. Muroga, K. Araki, M. Kiritani, J. Nucl. Mater. 179 (1991) 1078.
[5] P.B. Hirsch, Point defect cluster hardening, in: R.E. Smallman, J.E. Harris (Eds.), Vacancies, vol. 76, 1976.
[6] P. Scott, J. Nucl. Mater. 211 (1994) 101.
[7] J.F. Williams, T.R. Mager, P. Spellward, J. Walmsley, M. Koyama, I. Suzuki, H. Mimaki, in: 8th International Symposium on Environmental Degradation of Materials in Nuclear Power Systems – Water Reactors, Amelia Island, FL, USA, August 10–14, 1997, p. 725.
[8] J.T. Busby, G.S. Was, E.A. Kenik, J. Nucl. Mater. 302 (2002) 20–40.
[9] S.M. Bruemmer, E.P. Simonen, P.M. Scott, P.L. Andresen, G.S. Was, J.L. Nelson, J. Nucl. Mater. 274 (1999) 299–314.
[10] S.M. Bruemmer, L.A. Charlot, E.P. Simonen, in: D. Cubicciotti, E.P. Simonen, R. Gold (Eds.), in: Proceedings 5th International Symposium Environmental Degradation of Materials in Nuclear Power Systems – Water Reactors, American Nuclear Society, La Grange Park, IL, 1992, pp. 821–826.
[11] K. Fukuya, M. Nakano, K. Fujii, T. Torimaru, J. Nucl. Sci. Technol. 41 (2004) 594–600.
[12] G.S. Was, P.L. Andresen, J. Metals 44 (1992) 8.
[13] G.S. Was, S.M. Bruemmer, J. Nucl. Mater. 216 (1994) 326–347.
[14] P.L. Andresen, F.P. Ford, S.M. Murphy, J.M. Perks, in: Proceedings 4th International Symposium on Environmental Degradation of Materials in Nuclear Power Systems – Water Reactors, Jekyll Island, GA, 1989, p. 1.
[15] C. Pokor, Y. Bréchet, P. Dubuisson, J.-P. Massoud, X. Averty, J. Nucl. Mater. 326 (2004) 30–37.
[16] S. Zinkle, P. Maziasz, R. Stoller, J. Nucl. Mater. 206 (1993) 266–286.
[17] J. Gan, G.S. Was, J. Nucl. Mater. 297 (2001) 161–175.
[18] B.H. Sencer, G.M. Bond, M.L. Hamilton, F.A. Garner, S.A. Maloy, W.F. Sommer, J. Nucl. Mater. 296 (2001) 112–118.
[19] N. Hashimoto, E. Wakai, J.P. Robertson, J. Nucl. Mater. 273 (1999) 95–101.
[20] D.J. Edwards, E.P. Simonen, S.M. Bruemmer, J. Nucl. Mater. 317 (2003) 13–31.
[21] N. Hashimoto, E. Wakai, J.P. Robertson, J. Nucl. Mater. 273 (1999) 95.
[22] G.M. Bond, B.H. Sencer, F.A. Garner, M.L. Hamilton, T.R. Allen, D.L. Porter, in: S.M. Bruemmer, P. Ford, G. Was (Eds.), in: 9th International Conference on Environmental Degradation of Materials in Nuclear Systems – Water Reactors, The Minerals, Metals and Materials Society, Pennsylvania, 1999, p. 1045.
[23] D. Edwards, F. Garner, E. Simonen, S. Bruemmer, Characterization of Neutron-Irradiated 300-Series Stainless Steels to Assess Mechanisms of Irradiation-Assisted Stress Corrosion Cracking, vol. 2, Core Components, EPRI, Palo Alto, CA, 2001, W04065-20.
[24] D.J. Edwards, E.P. Simonen, F.A. Garner, L.R. Greenwood, B.M. Oliver, S.M. Bruemmer, J. Nucl. Mater. 317 (2003) 32.
[25] E.A. Kenik, K. Hojou, J. Nucl. Mater. 191–194 (1992) 1331.
[26] Y. Isobe, M. Sagisaka, F.A. Garner, S. Fujita, T. Okita, J. Nucl. Mater. 386–388 (2009) 661.
[27] A. Etienne, B. Radiguet, P. Pareige, J.-P. Massoud, C. Pokor, J. Nucl. Mater. 382 (2008) 64.
[28] J. Chaumont, F. Lalu, M. Salomé, Nucl. Instrum. Method. 189 (1981) 193.
[29] J.M. Martin, G. González-Díaz, Nucl. Instrum. Method. B 88 (1994) 331.
[30] J.F. Ziegler, J.P. Biersack, U. Littmark, The stopping and range of ions in solids, Pergamon Press, New York, 1985.
[31] G.H. Kinchin, R.S. Pease, Rep. Prog. Phys. 18 (1955) 1.
[32] D. Blavette, A. Bostel, J.M. Sarrau, B. Deconihout, A. Menand, Nature 363 (1993).
[33] B. Gault, F. Vurpillot, A. Vella, M. Gilbert, A. Menand, D. Blavette, B. Deconihout, Rev. Sci. Instrum. 77 (2006) 043705.
[34] A. Etienne, M. Hernández-Mayoral, C. Genevois, B. Radiguet, P. Pareige, J. Nucl. Mater. 400 (2010) 56–63.
[35] D.J. Edwards, A. Schemer-Kohrn, S. Bruemmer, Characterization of Neutron-Irradiated 300-Series Stainless Steels, EPRI, Palo Alto, CA, 2006, 1009896.
[36] T.R. Allen, J.I. Cole, C.L. Trybus, D.L. Porter, H. Tsai, F. Garner, E.A. Kenik, T. Yoshitake, J. Ohta, J. Nucl. Mater. 348 (2006) 148.
[37] G.S. Was, T.R. Allen, J. Nucl. Mater. 205 (1993) 332–338.